


## RESEARCH ARTICLE

# Degeneration of biological heart valve grafts in a rat model of superoxide dismutase-3 deficiency

Alexander Assmann<sup>1</sup>  | Vera Schmidt<sup>1</sup> | Caroline Lepke<sup>1</sup> | Yukiharu Sugimura<sup>1</sup> | Anna Kathrin Assmann<sup>1</sup> | Mareike Barth<sup>1</sup> | Artur Lichtenberg<sup>1,2</sup> | Payam Akhyari<sup>1</sup>

<sup>1</sup>Department of Cardiac Surgery and Research Group for Experimental Surgery, Heinrich Heine University, Medical Faculty, Düsseldorf, Germany

<sup>2</sup>CARID-Cardiovascular Research Institute Düsseldorf, Heinrich Heine University, Medical Faculty, Düsseldorf, Germany

**Correspondence**

Artur Lichtenberg, Department of Cardiac Surgery, Heinrich Heine University, Moorenstr. 5, 40225 Düsseldorf, Germany.

Email: [artur.lichtenberg@med.uni-duesseldorf.de](mailto:artur.lichtenberg@med.uni-duesseldorf.de)

**Funding information**

NA

**Abstract**

While oxidative stress is known as key element in the pathogenesis of atherosclerosis and calcific aortic valve disease, its role in the degeneration of biological cardiovascular grafts has not been clarified yet. Therefore, the present study aimed to examine the impact of oxidative stress on the degeneration of biological cardiovascular allografts in a standardized chronic implantation model realized in rats exhibiting superoxide dismutase 3 deficiency (SOD3<sup>(-)</sup>). Rats with SOD3 loss-of-function mutation ( $n = 24$ ) underwent infrarenal implantation of cryopreserved valved aortic conduits, while SOD3-competent recipients served as controls ( $n = 28$ ). After a follow-up period of 4 or 12 weeks, comparative analyses addressed degenerative processes, hemodynamics, and evaluation of the oxidative stress model. SOD3<sup>(-)</sup> rats presented decreased circulating SOD activity ( $p = .0079$ ). After 12 weeks, 58% of the implant valves in SOD3<sup>(-)</sup> rats showed regurgitation (vs. 31% in controls,  $p = .2377$ ). Intima hyperplasia and chondro-osteogenic transformation contributed to progressive graft calcification ( $p = .0024$ ). At 12 weeks, hydroxyapatite deposition ( $p = .0198$ ) and the gene expression of runt-related transcription factor-2 (Runx2) ( $p = .0093$ ) were significantly enhanced in group SOD3<sup>(-)</sup>. This study provides the first in vivo evidence that impaired systemic antioxidant activity contributes to biological cardiovascular graft degeneration.

**KEYWORDS**

aortic valve graft, calcification, graft degeneration, oxidative stress, superoxide dismutase-3

## 1 | INTRODUCTION

Oxidative stress has been shown to be involved in the pathogenesis of different entities of degenerative cardiovascular disease. In the context of atherosclerosis, oxidative stress contributes to vascular smooth muscle and endothelial cell activation, monocyte infiltration, lipid

oxidation and uptake, thrombosis, and thereby plaque formation and endothelial dysfunction.<sup>1</sup> Furthermore, clinically relevant risk factors of atherosclerosis, such as diabetes mellitus, hypertension, hypercholesterolemia, and smoking, are known to induce reactive oxygen species (ROS) generation, underlining the significance of oxidative stress as pathomechanism.<sup>2</sup>

This is an open access article under the terms of the [Creative Commons Attribution-NonCommercial-NoDerivs](https://creativecommons.org/licenses/by-nc-nd/4.0/) License, which permits use and distribution in any medium, provided the original work is properly cited, the use is non-commercial and no modifications or adaptations are made.

© 2022 The Authors. *The FASEB Journal* published by Wiley Periodicals LLC on behalf of Federation of American Societies for Experimental Biology.

Calcific aortic valve disease (CAVD) shares the mentioned risk factors of atherosclerosis. Thus, it is not surprising that calcified stenotic human aortic valves have been reported to exhibit increased ROS levels, particularly superoxide, in the presence of reduced antioxidant activity of superoxide dismutase (SOD) and catalase.<sup>3,4</sup> Oxidative stress induction in human valvular interstitial cells resulted in higher rates of apoptosis and increased gene expression of osteogenic markers if the cells originated from calcified stenotic valves, and addition of SOD to the experiment counteracted the pro-osteogenic effect.<sup>4</sup> While the adverse influence of ROS and the protective role of SOD have been demonstrated in the context of CAVD development, the role of oxidative stress in the degeneration of biological heart valve grafts is yet unclear. Research on this topic is all the more required, since surgical or interventional heart valve replacement is one of the most frequent cardiac procedures with an increasing number of currently far more than 300 000 annual cases worldwide and a dramatic impact on patients' morbidity, mortality, and health-related quality of life.<sup>5</sup>

SOD is the key antioxidant enzyme that catalyzes the reaction of superoxide anions to hydrogen peroxide. In mammals, three types of SOD have been identified: a primarily cytoplasmic (SOD1) and an extracellular membrane-bound (SOD3) copper-zinc isoform, as well as a mitochondrial manganese form (SOD2).<sup>6</sup> For SOD3, a rat model with loss-of-function mutation resulting in enzyme deficiency (SOD3<sup>E124D</sup>) has been developed.<sup>7</sup> Previous studies in the SOD3<sup>E124D</sup> model have shown enhanced endothelial dysfunction in the aorta,<sup>8</sup> and increased sensitivity to the development of pulmonary artery hypertension.<sup>7</sup>

The present study aimed to examine the impact of oxidative stress on the degeneration of biological cardiovascular allografts in a standardized, previously well-described chronic implantation model realized in rats exhibiting SOD3 deficiency.

## 2 | MATERIALS AND METHODS

### 2.1 | Animals

SOD3<sup>E124D</sup> (SS-Sod3<sup>m1Mcwi</sup>) rats exhibiting a homozygous loss-of-function mutation (G→T transversion in codon 124, leading to a glutamic acid to aspartic acid change) resulting in SOD3 deficiency (SOD3<sup>(-)</sup>)<sup>7</sup> and SOD3-competent controls without mutation were bred under license agreement with Transposagen Biopharmaceuticals Inc. (Lexington, KY, USA) in the local animal care facility of the University Duesseldorf, Germany. Both strains were initially obtained by backcrossing to a Dahl/salt-sensitive strain (SS/JrHsdMcwiCrI; purchased from Charles River

Laboratories International Inc., Wilmington, MA, USA), intercrossing and maintenance as homozygous colonies. The animals were fed ad libitum with a sodium-depleted diet (AIN 76A; Ssniff, Soest, Germany). All experiments as well as breeding were performed in agreement with the national animal welfare act and approved by the state animal care committee—reference numbers 84-02.04.2015.A207 and 84-02.04.2016.A495.

### 2.2 | Experimental design

For all experiments, male rats ( $n = 52$ , 24 in group SOD3<sup>(-)</sup> and 28 in group control) weighing 200 g to 250 g were used. After harvesting from Wistar donor rats, valved aortic conduits were cryopreserved for 4 weeks. Thereafter, the grafts were anastomosed to the infrarenal aorta of SOD3<sup>(-)</sup> or control rats, which had undergone interventional generation of native aortic valve insufficiency 2 weeks before. The recipient animals were followed up for a period of 4 or 12 weeks, after which the prostheses were explanted and prepared for the readout. A schematic workflow of the experiments including technical aspects and a timeline are presented in Figure 1.

All animal models, surgical techniques, the graft preparation, and the readout procedures were used or conducted according to standards previously established in our group.<sup>9–13</sup> In the following, brief descriptions are provided.

### 2.3 | Valved aortic conduit preparation

Valved aortic conduits were harvested from male Wistar donor rats. In brief, animals were euthanized, and U-shaped aortic conduits including the aortic valves were excised via sternotomy. After rinsing with heparinized phosphate-buffered saline (PBS), the grafts were transferred into the conservation medium (Dulbecco's modified Eagle's medium +10% dimethylsulfoxide +20% fetal calf serum at 5°C) and frozen to -80°C under controlled cooling (1°C per minute in a propan-2-ol box). Following 4 weeks of cryo-storage, the conduits were thawed, washed three times in heparinized PBS, and implanted in SOD3<sup>(-)</sup> or control rats.

### 2.4 | Conduit implantation and explantation

Fourteen days before graft implantation, all recipient rats underwent an echocardiography-controlled (Philips HDX 11 equipped with a 15 MHz probe, Amsterdam,

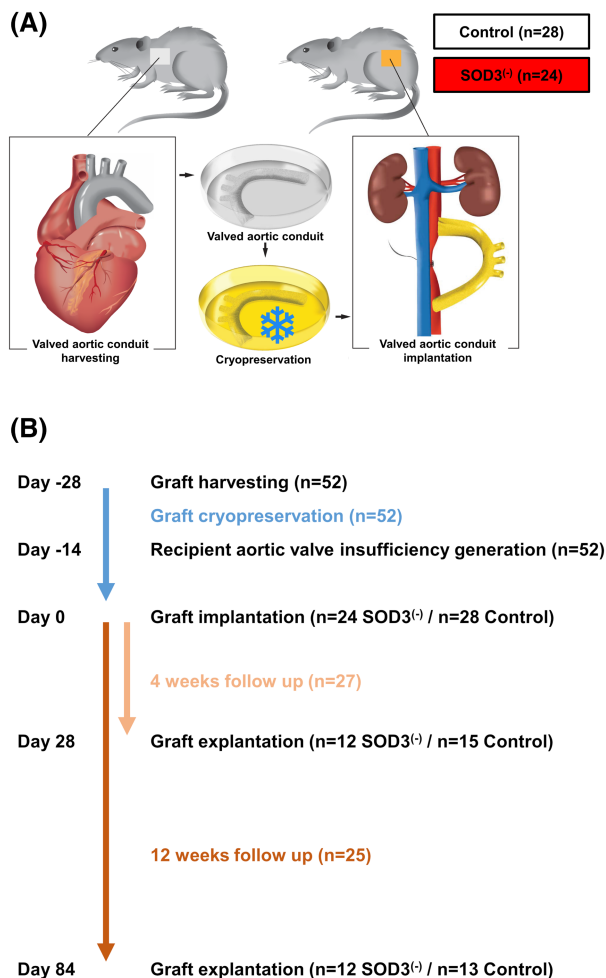


**FIGURE 1** Schematic presentation of technical aspects (A) and timeline (B) of the experiments. SOD3<sup>-/-</sup> rats with superoxide dismutase-3 deficiency. The schematic “A” is a modified reprint from Biomaterials 34(25); Assmann A, Delfs C, Munakata H, Schiffer F, Horstkötter K, Huynh K, Barth M, Stoldt VR, Kamiya H, Boeken U, Lichtenberg A, Akhyari P; Acceleration of autologous in vivo recellularization of decellularized aortic conduits by fibronectin surface coating; 6015–6026; 2013, with permission from Elsevier.

Netherlands) interventional generation of native aortic valve insufficiency (grade II-III) by guide-wire-induced leaflet perforation via the right common carotid artery under general inhalative anesthesia (isoflurane 2.0%–2.5%). The severity of insufficiency was assessed by Doppler sonography with a calculation of the RVTI (ratio of velocity time integrals = blood velocity-time integral of diastolic retrograde flow divided by blood velocity-time integral of antegrade flow) in the ascending aorta.

Valved aortic conduit implantation was also carried out under anesthetization with isoflurane (2.0%–2.5%) via an endotracheal tube and analgesia with subcutaneous carprofen (5 mg × kg<sup>-1</sup> body weight). Following a

standardized microsurgical protocol, midline laparotomy was conducted, the intestines were mobilized, and the infrarenal aorta was separated from the vena cava. Systemic heparinization (300 IU × kg<sup>-1</sup> body weight) via a central venous catheter in the right jugular vein was followed by infrarenal aortic clamping. The proximal and distal anastomoses with the U-shaped conduit were sutured in an end-to-side manner with continuous suture lines (polypropylene 10-0, Ethicon, Norderstedt, Germany). Ligation of the native aorta between the two anastomoses was conducted to improve the graft perfusion and valve motion, which were controlled by Doppler sonography—including RVTI assessment distally of the implant—after abdominal closure.

After 4 or 12 weeks of follow-up, the rats were anesthetized again, and Doppler sonography was conducted to control graft perfusion and valve motion, whereat any degree of valve regurgitation was considered significant. Median laparotomy was followed by excision of the prostheses and processing for further readout.

## 2.5 | Histology

For histomorphological analyses of the explants, cryosections (5 μm thick) were generated and stained with hematoxylin/eosin, or according to von Kossa or Movat pentachrome protocols. Quantification of intima hyperplasia, graft calcification, and chondrogenic remodeling was performed by standardized scoring systems as described below. Analyses were carried out in cross-sections from four defined graft regions: proximal anastomosis, ascending aorta, descending aorta, and distal anastomosis. Each cross-section was further divided into eight equal segments for quantitative assessment.

The thicknesses of intima and media were measured in hematoxylin/eosin staining to calculate the intima/media ratio.

The amount of intima and media calcification was assessed by a semi-quantitative score based on von Kossa staining and ranging from 0 to 5: 0 = no calcification; 1 = micro-calcification; 2 = macro-calcification <25% of the tissue area; 3 = macro-calcification <50% of the tissue area; 4 = macro-calcification <75% of the tissue area; 5 = macro-calcification >75% of the tissue area.

The area of chondrogenic remodeling in the intima and media was quantified based on Movat pentachrome staining with scores ranging from 0 to 5: 0 = no chondrogenic remodeling; 1 = sparse spots of chondrogenic remodeling; 2 = chondrogenic remodeling <25% of the tissue area; 3 = chondrogenic remodeling <50% of the tissue area; 4 = chondrogenic remodeling <75% of the tissue area; 5 = chondrogenic remodeling >75% of the tissue area.

## 2.6 | Quantitative RNA analysis

By means of quantitative real-time detection polymerase chain reaction (RTD-PCR), the expression of specific genes in the explanted grafts was analyzed. Total ribonucleic acid (RNA) was isolated applying a standard guanidinium thiocyanate-phenol-chloroform extraction (TRIzol) method and a commercially available isolation kit (RNeasy Mini Kit; Qiagen, Hilden, Germany). In brief, after tissue homogenization in TRIzol (Invitrogen, Carlsbad, CA, USA), RNA was precipitated by isopropanol. Passage through a deoxyribonucleic acid (DNA)-removing column (Qiagen, Hilden, Germany) was followed by RNA sample collection and quantity analysis in an Infinite M1000 pro microplate reader (Tecan, Maennedorf, Switzerland). RNA integrity assessment was conducted using the Agilent RNA 6000 Nano Kit (Agilent Technologies, Santa Clara, CA, USA). For cDNA generation, the QuantiTect Reverse Transcription Kit (Qiagen, Hilden, Germany) was utilized according to the manufacturer's protocol. Quantitative RTD-PCR was conducted on a StepOnePlus cycler (Applied Biosystems, Foster City, CA, USA) using the GoTaq qPCR Master Mix (Promega, Madison, WI, USA). Relative gene expression was calculated using the delta-delta Ct method. Primers for the following genes were obtained from Eurofins Genomics (Louisville, KY, USA): runt-related transcription factor-2 (Runx2), osteopontin, alpha-smooth muscle actin ( $\alpha$ SMA), interleukin-1-beta (IL1 $\beta$ ), transforming growth factor-beta (TGF $\beta$ ), tumor necrosis factor-alpha (TNF $\alpha$ ), superoxide dismutase-1 (SOD1), and superoxide dismutase-3 (SOD3). All primer sequences are displayed in Table S1.

## 2.7 | Oxidative stress assays

Total SOD activity in the blood serum as well as in homogenized samples of the native aorta was assessed by means of a tetrazolium salt-based colorimetric assay kit (Cayman Chemical, Ann Arbor, MI, USA) according to the manufacturer's protocol. For specific measurement of SOD2 activity, copper-zinc SOD (SOD1 and SOD3) activity was blocked by the addition of 2 mM potassium cyanide. All SOD activity values were normalized to the protein content of the respective samples, assessed by means of the Bicinchoninic Acid Protein Assay Kit (Sigma-Aldrich, Taufkirchen, Germany) according to the manufacturer's protocol, and the mean value of the total SOD activity of the respective control group.

Detection of ROS in the native aorta was conducted by a modified lucigenin-mediated chemiluminescence approach.<sup>14</sup> Aortic rings (2 mm thick) were placed in sterile Krebs-HEPES (4-[2-hydroxyethyl]-1-piperazineethanesulfonic acid) buffer (Noxygen, Elzach, Germany) at 37°C in the dark. After the addition of 50  $\mu$ M lucigenin (Santa Cruz

Biotechnology, Dallas, TX, USA), luminescence was measured every minute for a total of 30 min and normalized to the tissue dry weight and the mean value of the control group.

Absorption in the SOD activity assay and luminescence in the ROS detection assay were measured on an Infinite M1000 pro microplate reader (Tecan, Maennedorf, Switzerland).

## 2.8 | Statistics

Data are presented as median and interquartile range (IQR) for all continuous variables. Following normality testing (D'Agostino-Pearson test), direct group comparisons were conducted by two-tailed Mann-Whitney-U tests or two-tailed Student's *t*-tests, respectively. Group comparisons over time were evaluated by two-way analyses of variance. Statistical significance was assigned to *p*-values lower than .05. Data analysis was performed with Graph Pad Prism v6.01 (Graph Pad Software, San Diego, CA, USA).

## 3 | RESULTS

### 3.1 | SOD3 deficiency model

SOD3<sup>(-)</sup> rats exhibited significantly reduced total serum SOD activity when compared to controls (0.32 [IQR, 0.28–0.44] vs. 0.82 [IQR, 0.75–1.34], *p* = .0079) (Figure 2A). Neither the total SOD activity (*p* = .9444) nor the SOD2 activity (*p* = .9444) in the aortic wall differed between SOD3<sup>(-)</sup> and control animals (Figure 2B). The amount of ROS in aortic wall tissue was similar in both groups (*p* = .6571) (Figure 2C). Gene expression of SOD1 was significantly enhanced in the aortic wall of group SOD3<sup>(-)</sup> (*p* = .0110), and considering SOD1 and SOD3 together, the expression in group SOD3<sup>(-)</sup> was increased as compared to controls (“group” as source of variation: *p* = .0033) (Figure 2D). A comparison of the gene expression of SOD1 and SOD3 in valved aortic conduit explants did not reach statistically significant differences between group SOD3<sup>(-)</sup> and controls when calculated for each gene separately (SOD1: *p* > .9999; SOD3: *p* = .1276), however, considering both genes together, group SOD3<sup>(-)</sup> showed increased expression as compared to controls (“group” as source of variation: *p* = .0468) (Figure 2E).

### 3.2 | Hemodynamic outcome

Animals that deceased in the experiments and thus could not be included in the analyses are listed in Table S2.

Echocardiography showed equal severities of the generated native aortic valve insufficiency in the SOD3<sup>(-)</sup>

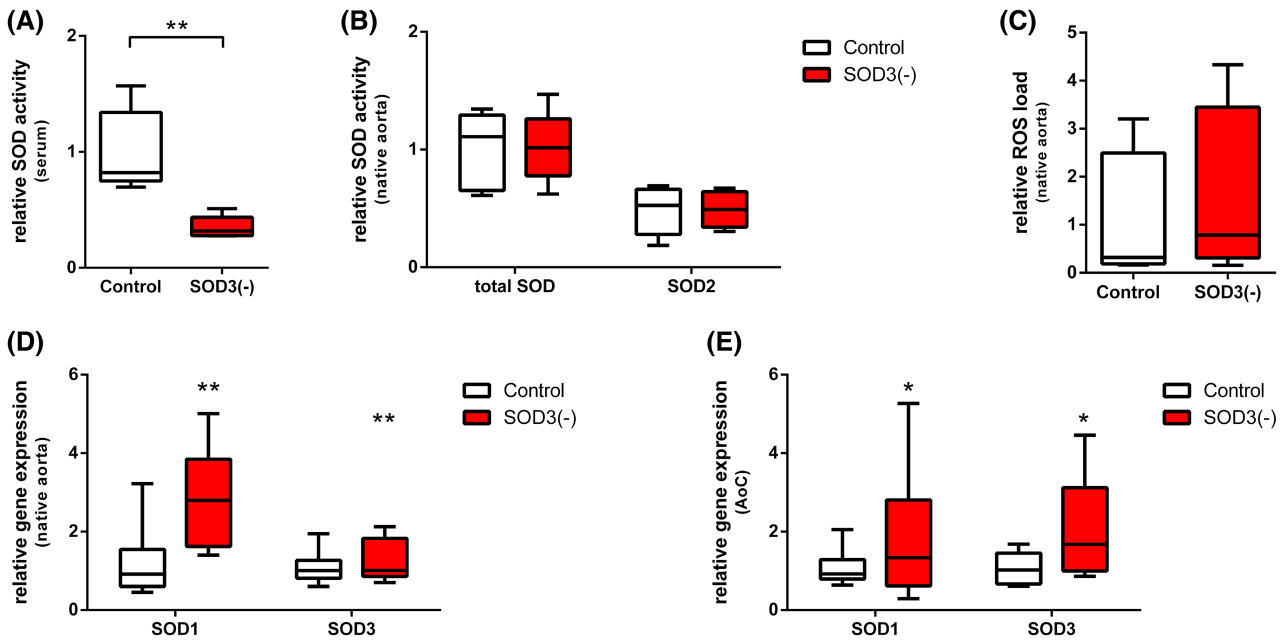


**FIGURE 2** SOD3 deficiency model. Total SOD activity in the blood serum (A), and SOD activity in the native aorta (B). ROS detection in the native aorta (C). SOD gene expression in the native aorta (D) and in valved aortic conduits (E). \* $p < .05$ , \*\* $p < .01$  (in D and E for SOD3<sup>-/-</sup> vs. Control when considering the genes SOD1 and SOD3 together). Upper and lower box margins represent 25% and 75% intervals, respectively, with whiskers representing minimum and maximum values. AoC, valved aortic conduit; ROS, reactive oxygen species; SOD, superoxide dismutase; SOD3<sup>-/-</sup>, rats with superoxide dismutase-3 deficiency.

and control group (RVTI 0.73 [IQR, 0.64–0.85] vs. 0.68 [IQR, 0.59–0.77],  $p = .2601$ ) directly after generation. Furthermore, the severity of insufficiency resulting in retrograde diastolic flow in the aorta remained stable during the whole study period (SOD3<sup>-/-</sup> vs. controls: RVTI at 4 weeks  $p = .2558$ , RVTI at 12 weeks  $p = .2865$ ; “time” as source of variation:  $p = .1943$ ) (Figure 3A).

Twelve weeks after implantation, Doppler sonography revealed an insufficiency of the implanted aortic conduit valve in 58% of the rats in group SOD3<sup>-/-</sup>, while only 31% of the control animals exhibited any valvular regurgitation in the graft ( $p = .2377$ ) (Figure 3B). The severity of conduit valve insufficiency was determined by assessment of the RVTI distally of the implant. While directly after implantation, no regurgitation was present in either group, conduit valve insufficiency developed over time ( $p < .0001$ ), however, without a statistically significant difference between the two groups (SOD3<sup>-/-</sup> vs. controls: RVTI at 4 weeks  $p = .4656$ , RVTI at 12 weeks  $p = .3964$ ; “group” as source of variation:  $p = .1256$ ) (Figure 3C).

### 3.3 | Graft degeneration

All grafts showed signs of hyperplastic intima formation (Figure 4A–D). The mean intima thickness presented with enhanced but not significantly increased values in group SOD3<sup>-/-</sup> (at 4 weeks: 25.8  $\mu\text{m}$  [IQR 13.3–86.0  $\mu\text{m}$ ] vs. 28.0  $\mu\text{m}$

[IQR 11.0–50.1  $\mu\text{m}$ ] in controls, at 12 weeks: 40.6  $\mu\text{m}$  [IQR 16.2–75.1  $\mu\text{m}$ ] vs. 30.6  $\mu\text{m}$  [IQR 14.5–57.1  $\mu\text{m}$ ], “group” as source of variation:  $p = .0979$ ). Calculation of the intima/media ratios resulted in similar amounts of intima hyperplasia in both groups at all time points (“group” as source of variation:  $p = .3164$ ) (Figure 4E).

Aortic wall areas with chondrogenic remodeling, exhibiting cells with chondroid phenotype and surrounding glycosaminoglycan accumulation, occurred in the graft media as well as in hyperplastic intima regions. In the media, these areas seemed to be more frequent in explants of group SOD3<sup>-/-</sup> (Figure 5A–D). However, quantitative Movat staining-based analysis just failed to reach statistical significance (“group” as source of variation:  $p = .0686$ ) (Figure 5E). In the intima, the amount of chondrogenic remodeling was similar in both groups (“group” as source of variation:  $p = .2998$ ).

The graft media of SOD3<sup>-/-</sup> rats presented with progressive hydroxyapatite deposition over time ( $p = .0024$ ) (Figure 6A–D), which reached significantly increased values at 12 weeks when compared to controls (1.56 [IQR 0.78–1.97] vs. 0.94 [IQR 0.53–1.47],  $p = .0198$ ) (Figure 6E). In the intima, the extent of calcification was similar in both groups ( $p = .5131$  at 4 weeks;  $p = .6053$  at 12 weeks). Gene expression analyses revealed significantly increased Runx2 levels in SOD3<sup>-/-</sup> rats at 12 weeks (1.66 [IQR 1.35–3.41] vs. 0.93 [IQR 0.81–1.17] in controls,  $p = .0093$ ) (Figure 6F). Osteopontin (1.30

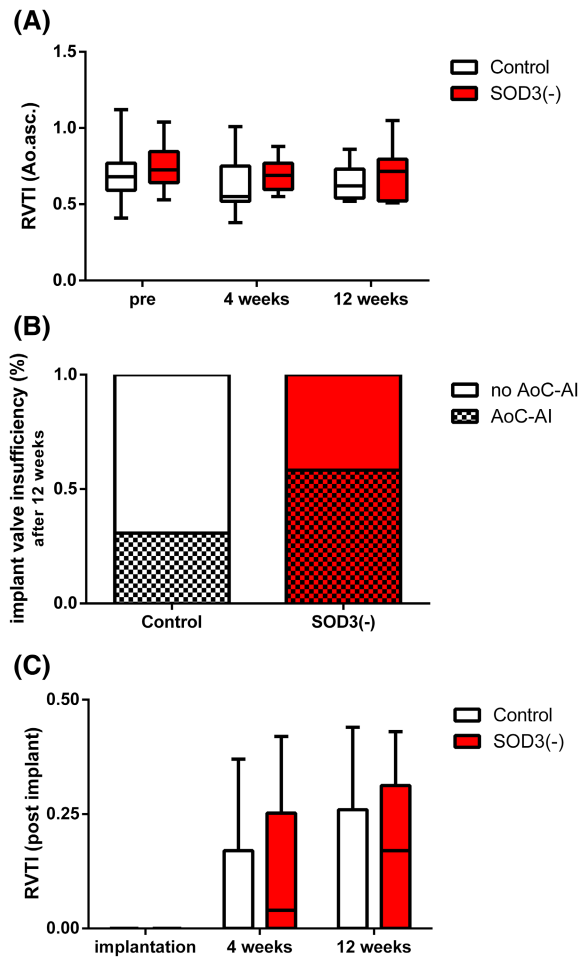


**FIGURE 3** Hemodynamic outcome. Time course of the severity of native aortic valve insufficiency (A). Development of aortic conduit valve insufficiency by week 12 (B). Time course of the severity of aortic conduit valve insufficiency (C). Upper and lower box margins (in A and C) represent 25% and 75% intervals, respectively, with whiskers representing minimum and maximum values. Ao.asc., ascending aorta; AoC-AI, insufficiency of the aortic conduit valve; pre, directly before AoC implantation; RVTI, ratio of velocity time integrals; SOD3<sup>(-)</sup>, rats with superoxide dismutase-3 deficiency.

[IQR 0.77–3.17] vs. 1.12 [IQR 0.76–1.39],  $p = .1843$ ) and  $\alpha$ SMA (1.33 [IQR 1.06–2.47] vs. 1.08 [IQR 0.66–1.80],  $p = .1514$ ) showed slightly elevated gene expression without statistical significance.

The inflammatory markers Il1 $\beta$  ( $p = .6126$ ), TGF $\beta$  ( $p = .9889$ ) and TNF $\alpha$  ( $p = .2810$ ) were not differently expressed in the two study groups (Figure S1).

## 4 | DISCUSSION

### 4.1 | Oxidative stress animal model

Animal models of enhanced oxidative stress are generated by either increased ROS generation or decreased

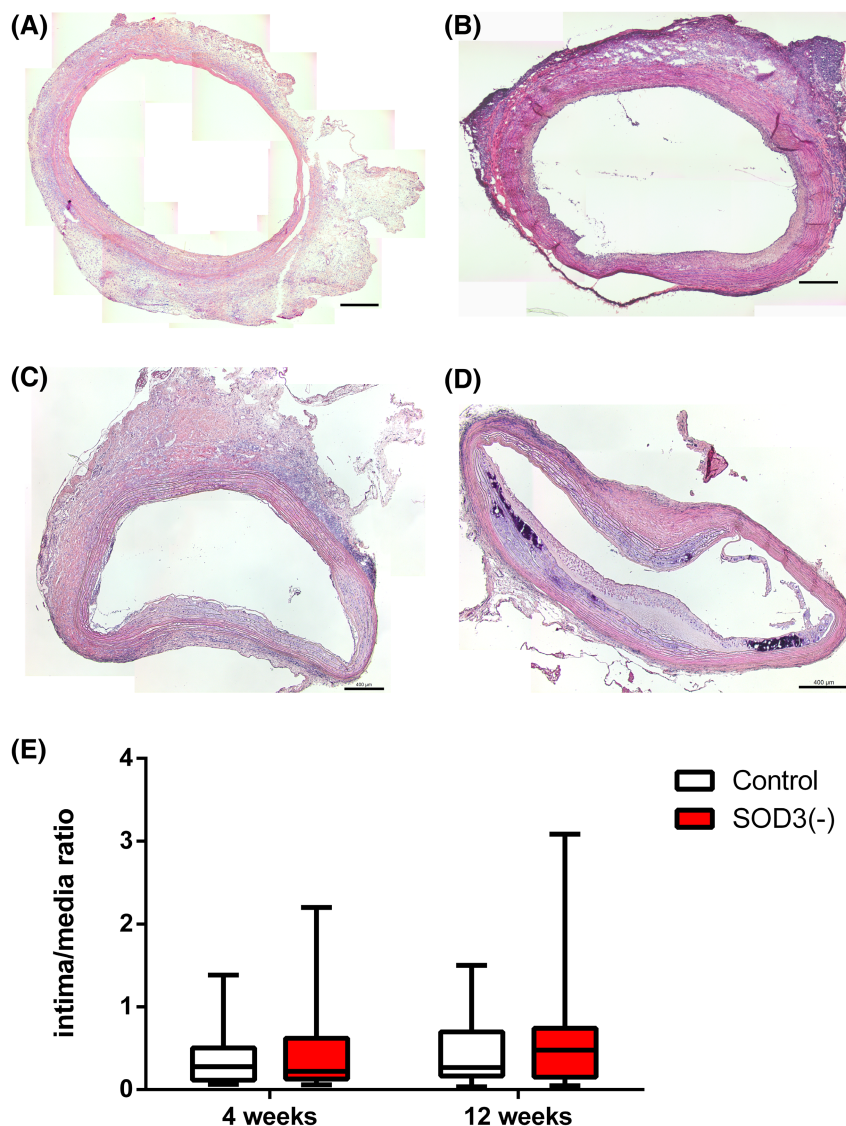
ROS inactivation. Impairment of ROS inactivation can be achieved by reduction of the SOD activity, resulting in superoxide anion accumulation. In mice, genetical modifications have led to strains with deficiency of specific SOD isoforms.<sup>15</sup> In humans, loss-of-function mutations in the SOD genes do not seem to play a major role, however, the common SOD3 gene variant SOD3<sup>R213G</sup> impairs the binding of SOD3 to the cellular surface by modification of the heparin-binding domain in humans.<sup>16</sup> SOD3<sup>R213G</sup> has been found to be associated with enhanced risk of ischemic heart disease,<sup>17</sup> increased mortality from ischemic heart disease in diabetic patients on hemodialysis,<sup>18</sup> and in contrast to regular SOD3, an experimental upregulation of SOD3<sup>R213G</sup> did not protect against endothelial dysfunction in the context of hypertension or heart failure.<sup>19,20</sup> Interestingly, the adverse effects of SOD3<sup>R213G</sup> on the course of myocardial ischemia were observed only in patients aged >70 years, which parallels findings in SOD3-deficient mice that SOD3 activity is important to protect from endothelial dysfunction, particularly in old animals.<sup>21</sup> These observations speak in favor of pathophysiological mechanisms that either require disease scenarios with high oxidative stress levels or accumulation over time to result in clinically manifest disease. The existing data on SOD3<sup>R213G</sup> confirm that animal models of SOD3 deficiency mimic clinically relevant cardiovascular disease scenarios.

Due to technical limitations inherent to the microsurgical model, the mentioned genetically modified mouse models are not suitable for the implantation of valved aortic conduits. A rat model of SOD3 deficiency (SOD3<sup>E124D</sup> Dahl/SS background-based strain) has been reported to exhibit increased aortic sensitivity to phenylephrine and reduced relaxation to acetylcholine when compared to SOD3-competent controls.<sup>8</sup> Furthermore, this strain presents exacerbated monocrotaline-induced pulmonary hypertension, pulmonary vascular remodeling, right ventricular hypertrophy, and right ventricular fibrosis as compared to controls.<sup>7</sup> In lung tissue of SOD3<sup>E124D</sup> rats, the total SOD activity was slightly decreased. Both studies demonstrate pro-degenerative effects of the loss-of-function mutation on the vasculature of rats. Therefore, we have decided to combine our established modular model of cardiovascular graft implantation into the systemic circulation with the SOD3<sup>E124D</sup> rat model.<sup>9,13</sup>

Only male rats have been included in our study to avoid potential effects of the female hormone cycle on graft degeneration, such as estrogen-dependent protection from cardiovascular calcification. Relevant gender effects have been shown in arterial and valvular calcification as well as in structural aortic valve graft degeneration.<sup>22,23</sup>

SOD3<sup>E124D</sup> animals in our study showed significantly decreased total SOD activity in the blood serum, which

**FIGURE 4** Graft intima hyperplasia. Representative images of hyperplastic intima formation 4 weeks (A, B) and 12 weeks (C, D) after implantation in SOD3<sup>(-/-)</sup> rats (B, D) or controls (A, C). Quantification of the graft intima hyperplasia (E). Hematoxylin/eosin staining. Scale bars = 400 μm. Upper and lower box margins represent 25% and 75% intervals, respectively, with whiskers representing minimum and maximum values. SOD3<sup>(-/-)</sup> rats with superoxide dismutase-3 deficiency.



is explained by the fact that SOD3 is the most frequent SOD isoform in extracellular fluids including blood.<sup>24</sup> On the contrary, the total SOD activity and the SOD2 activity in the aortic wall did not differ between SOD3-deficient and SOD3-competent animals. In line with these results, the ROS load in the aortic wall was not significantly enhanced in the SOD3<sup>(-/-)</sup> group. Intracellular SOD activity in the aortic wall originates from SOD1 and SOD2, while interstitial activity is attributed to the action of SOD3. The finding that SOD2 and total SOD activity were similar in both groups suggests that either SOD3 did not relevantly contribute to the total SOD aortic activity in our rat model, so that the loss of function in the SOD3<sup>(-/-)</sup> group did not influence this parameter, or the SOD3 deficiency resulted in compensatory upregulation of the SOD1 activity.

The first hypothesis of low contribution of SOD3 to the aortic wall SOD activity is supported by the observation that rats have a low endothelial binding

affinity of SOD3 and thus low tissue concentrations.<sup>25</sup> Nevertheless, we have observed a trend toward compensatory overexpression of SOD1 and dysfunctional SOD3 in the valved conduit explants, both of which are copper-zinc SOD isoforms. Maybe, the difference did not reach statistical significance due to low animal numbers. It speaks in favor of compensatory mechanisms that a previous study on the SOD3<sup>E124D</sup> model revealed a remarkable SOD activity increase in the resistance arteries as compared to SOD3-competent animals.<sup>8</sup> Interestingly, the gene expression of SOD1, SOD2, and SOD3 was not significantly changed. These data are confirmed by experiments in mice with genetical SOD3 deficiency and related upregulated copper-zinc SOD activity and preserved vascular function during angiotensin-II-induced hypertension.<sup>26</sup> Again, the upregulation of SOD activity was not accompanied by an increase in copper-zinc SOD protein expression. As underlying mechanisms,

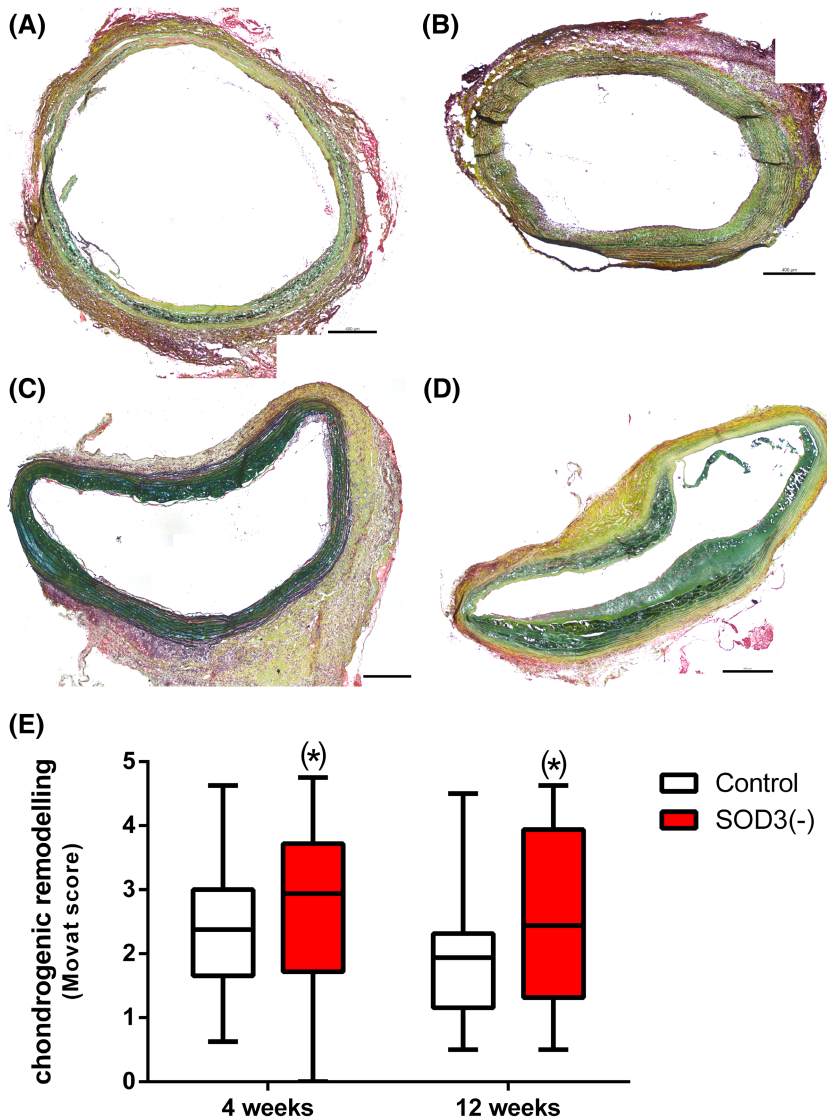


**FIGURE 5** Chondrogenic graft remodeling. Representative images of chondroid tissue degenerative 4 weeks (A, B) and 12 weeks (C, D) after implantation in SOD3<sup>(-)</sup> rats (B, D) or controls (A, C). Scoring of the chondrogenic graft area (E). Movat pentachrome staining. Scale bars = 400 μm. (\**p* = .0686 (for SOD3<sup>(-)</sup> vs. Control when considering both time points together). Upper and lower box margins represent 25% and 75% intervals, respectively, with whiskers representing minimum and maximum values. SOD3<sup>(-)</sup>, rats with superoxide dismutase-3 deficiency.

an upregulation of the copper chaperone protein for copper-zinc SOD and a restoration of the ROS-depleted enzyme copper levels were proposed. An actual compensatory increase in SOD1 activity in SOD3<sup>E124D</sup> animals may be masked by the fact that the tetrazolium salt-based colorimetric assay used in the present study does not allow for differentiation between SOD1 and SOD3 activity, since potassium cyanide inhibits the activity of both copper-zinc SOD isoforms. Therefore, despite not significantly enhanced gene expression, the SOD1 activity in SOD3<sup>E124D</sup> animals might be increased compared to SOD3-competent rats.

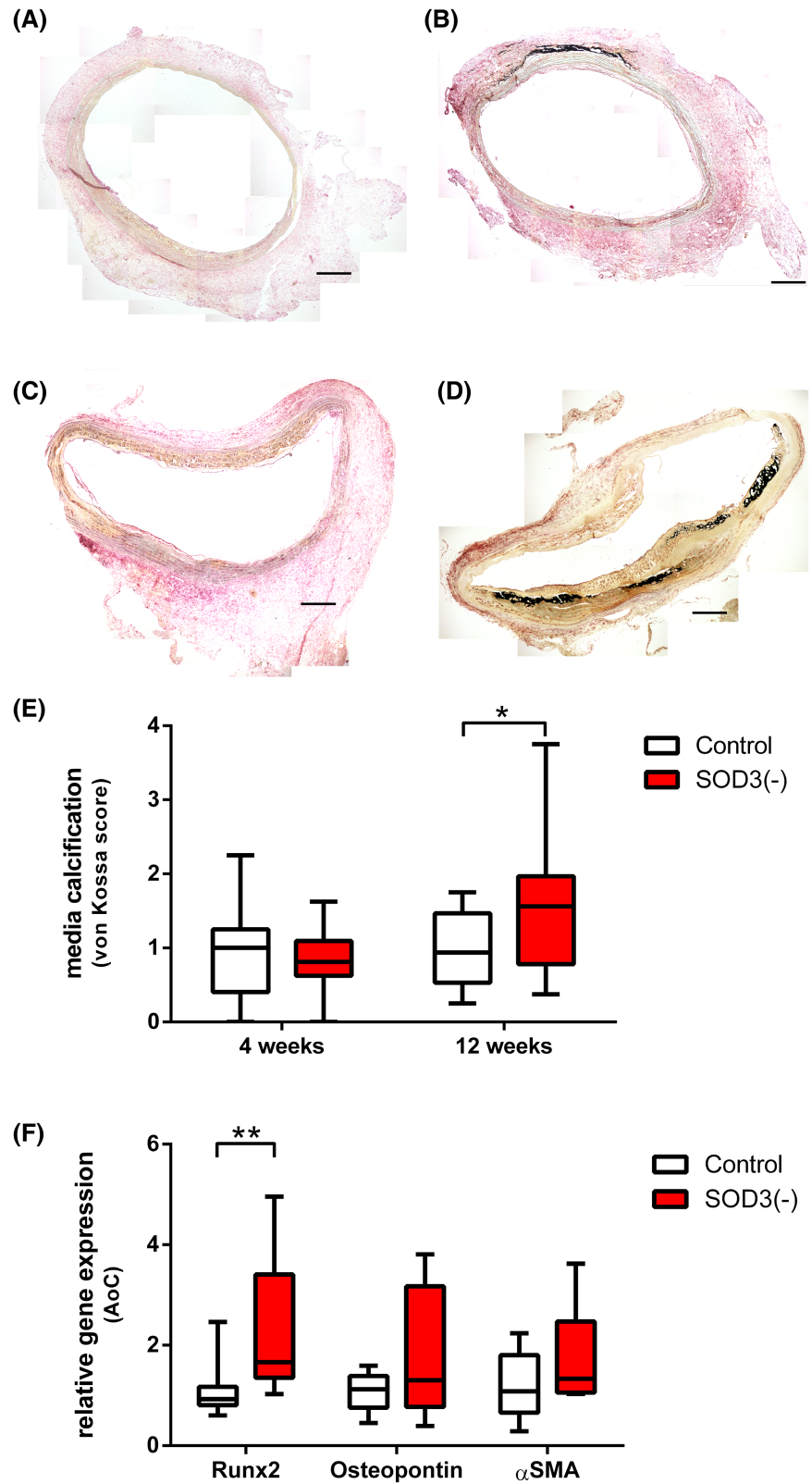
In summary, the SOD3<sup>E124D</sup> model provides significantly decreased antioxidant SOD activity in circulating blood, whereas the actual impact on degenerative processes in the aortic wall, and thus in aortic conduit grafts, might be attenuated due to either low significance of SOD3 in the rat aortic wall or potential protective upregulation of the local copper-zinc isoform SOD1.

## 4.2 | Valved aortic conduit degeneration

Advanced stages of native aortic valve degeneration necessitate surgical or interventional heart valve replacement. Our aging societies exhibit increasing numbers of elderly patients with aortic valve deterioration, and timely valve replacement results in significant improvement of morbidity, mortality, and health-related quality of life,<sup>27</sup> both underlining the epidemiological significance of heart valve grafting. Since graft failure requires complex redo procedures with enhanced risk of morbidity and mortality,<sup>28</sup> research on the elucidation of degenerative processes as potential targets for supportive therapies to improve the durability of heart valve grafts is of major interest.

The revelation of mechanisms of prosthesis degeneration is all the more crucial, as personalized medicine has come into the focus of clinical therapy as well as science. Based on the understanding of the processes leading to

**FIGURE 6** Graft calcification. Representative images of degenerative aortic conduit calcification 4 weeks (A, B) and 12 weeks (C, D) after implantation in SOD3<sup>(-)</sup> rats (B, D) or controls (A, C). Scoring of the hydroxyapatite deposition (E). Gene expression of markers of osteogenic transformation (F). von Kossa staining. Scale bars = 400 μm. \**p* < .05, \*\**p* < .01. Upper and lower box margins represent 25% and 75% intervals, respectively, with whiskers representing minimum and maximum values. αSMA, alpha-smooth muscle actin; AoC, valved aortic conduit; Runx2, runt-related transcription factor-2; SOD3<sup>(-)</sup>, rats with superoxide dismutase-3 deficiency.



graft deterioration, an individual decision on the type of graft for surgical or interventional heart valve replacement may be made, particularly in younger patients who regularly exhibit a complex genetical predisposition to cardiovascular degeneration.

Despite the aforementioned knowledge on the crucial role of oxidative stress in atherosclerosis and the adverse impact on CAVD progression, scientific reports on the role of oxidative stress in biological heart valve graft degeneration are sparse. A study on biological aortic valve

prostheses explanted due to graft failure has demonstrated an association between calcifying deterioration and elevated oxidized amino acids.<sup>29</sup> Biological heart valves have also been reported to be generally susceptible to collagen deterioration, loss of glutaraldehyde cross-links, and collagenase degradation under oxidizing *in vitro* conditions, the adverse effects of which can be counteracted by oxidant scavenging.<sup>30</sup> To the best of our knowledge, the present study is the first *in vivo* experiment addressing the impact of reduced antioxidant activity on the degeneration of biological heart valve grafts.

In order to allow for regular motion of the implanted aortic conduit valves, native aortic valve insufficiency grade II-III was interventionally generated prior to graft implantation as previously established.<sup>12</sup> Doppler sonography revealed equal severity of regurgitation in both study groups without a relevant change during the study period, so that the hemodynamic conditions for the grafts in both groups were steady over time. Directly after implantation, all implant valves presented with a normal motion without any regurgitation. After 12 weeks *in vivo*, some animals had developed regurgitation of the implanted aortic valve. The percentage of functionally impaired implanted aortic valve grafts was approximately twice as high in the SOD3<sup>(-)</sup> group when compared to controls (58% vs. 31%). Doppler sonography-based quantification showed a significant progress in the regurgitation severity over time. Due to the low animal number per group, neither the occurrence of regurgitation nor its quantified severity reached statistically significant inter-group differences, however, the results suggest a higher risk of early onset of graft degeneration under SOD3 deficiency conditions.

The implantation of cryopreserved valved aortic conduit grafts into the systemic circulation of recipients in the present study resulted in moderate adverse intima hyperplasia in both study groups. This finding confirms data from previous experiments on cryopreserved cardiovascular allografts implanted in rats, in which hyperplastic intima formation in the presence of activated myofibroblasts was detected.<sup>9,31,32</sup>

In areas of advanced intima hyperplasia, chondro-osteogenic transformation typically occurs. The presence of myofibroblasts undergoing a transformation toward chondroid cells in hyperplastic intima has been previously described in the herein applied cardiovascular graft implantation model.<sup>10,33</sup> In line with those observations, chondrogenic remodeling with chondroid cells and surrounding proteoglycan accumulation as well as hydroxyapatite deposition have been detected in hyperplastic intima regions in the present experiments, whereas no differences occurred between SOD3<sup>(-)</sup> and control animals.

In the graft media, similar processes of chondrogenic remodeling and calcium deposition were found. In contrast

to the intima, the media presented with pronounced chondroid remodeling and significantly increased calcification in SOD3-deficient animals when compared to controls. In line with these findings, Runx2 expression was enhanced in conduits from SOD3<sup>(-)</sup> rats, which confirms previous data on the role of Runx2 as osteogenic transcription factor promoting calcifying cardiovascular degeneration.<sup>9,34</sup> In particular, elevated Runx2 levels have been detected in valvular interstitial cells under pro-osteogenic stimulation.<sup>35</sup> Interestingly, the increase of Runx2 expression in that experiment was abrogated when valvular interstitial cells were co-cultured with valvular endothelial cells. These findings seem to support data from the present study, in which chondro-osteogenic remodeling occurred predominantly in the graft media where—in opposite to the implant intima—no endothelial cells are present.

Twelve weeks after implantation, valved aortic conduits from SOD3<sup>(-)</sup> and control rats exhibited similar gene expression of typical inflammatory markers, such as IL1 $\beta$ , TGF $\beta$ , and TNF $\alpha$ . Either inflammatory processes were not predominantly involved in the increased media calcification in SOD3-deficient animals, or their significance was not detected. The latter explanation may be caused either by the fact that gene expression analyses were conducted in whole explants, while differences in calcification occurred only in the graft media so that potential inter-group differences may be masked. Alternatively, it may be caused by the single analysis time point of 12 weeks, which might be too late since inflammation has been reported to be particularly involved in the early phase of cardiovascular degeneration.<sup>36</sup>

However, a comparison with different types of vascular calcification supports the hypothesis that inflammation was not crucially involved in graft degeneration in the present study. Aggravated chondro-osteogenic remodeling in SOD3-deficient rats was predominantly observed in the implant media. In native arteries, media calcification (“arteriosclerosis”) is known to be driven also by oxidative stress, while inflammation—in opposite to its significance in intima calcification (“atherosclerosis”)—does not play a major role.<sup>37</sup> Similar pathophysiological processes in arterial media calcification and biological heart valve graft calcification may explain the site of oxidative stress-aggravated degeneration, the implant media, as well as the minor influence of inflammation. Moreover, this may account for the finding that intima hyperplasia was not increased in SOD3-deficient rats.

### 4.3 | Study limitations

There are different potential explanations why SOD3<sup>E124D</sup> rats showed significantly increased implant

calcification, while analysis of other pro-degenerative parameters failed to show a statistically significant difference. One possible reason may be the duration of the follow-up period. In a previous study on the SOD3<sup>E124D</sup> model, development of chronic kidney disease, comprising focal necrosis and fibrosis, glomerulosclerosis, massive proteinaceous cast accumulation with tubular dilatation, interstitial fibrosis with hypertension, and renal failure with increased serum creatinine, was not present at 8 weeks, however, it became clinically relevant by week 21.<sup>38</sup> A low but continuous oxidative stress influence seems to be causal. As a consequence, studies on the in vivo degeneration of valved aortic conduits with follow-up periods beyond 12 weeks would be interesting.

Another explanation for moderate degenerative effects may be the choice of species for our animal model. The impact of SOD3 on vascular disease in rats has been questioned, since rats exhibit a low binding affinity of SOD3 to proteoglycans on the cellular surface, so that the interstitial SOD3 content in rat tissues including vascular walls is low compared to other mammals.<sup>25,39,40</sup> Despite this fact, our study revealed enhanced graft degeneration in SOD3<sup>E124D</sup> rats, and it can be speculated that the impact might be even higher in humans who exhibit larger amounts of SOD3 in the vascular wall tissue.

Additionally, it has to be mentioned that the intracellular SOD1 is supposed to be the primary regulator of superoxide levels in the vascular wall under normal conditions, while SOD3 may play a more important role under pathological conditions.<sup>41</sup> Since our SOD3<sup>E124D</sup> model under sodium-depleted diet is not a disease model with enhanced ROS generation, the reduction of extracellular antioxidant capacity by SOD3 deficiency may not be as crucial in terms of graft degeneration. Regarding this aspect, an additional disease model, such as hypertension induced by high-salt diet for the Dahl/SS-based SOD3<sup>E124D</sup> strain, would be a logical next step. Otherwise, for the present proof-of-concept study, our chosen design of diminished antioxidant capacity without additional ROS-enhancing disease has the advantage that no potential side effects of such a disease on graft degeneration have to be considered.

Furthermore, regarding the characterization of the SOD3 deficiency model, the size of the graft explants in our small animal model did not allow for additional ROS analyses beyond the conducted readout methods. Due to ethical concerns, we have not considered respective additional experiments—with animal numbers high enough for statistical comparisons—to be justified, particularly not since the ROS load in the nearby aortic wall was analyzed.

## 5 | CONCLUSIONS

The present study provides the first in vivo evidence that impaired antioxidant activity contributes to calcifying degeneration of biological cardiovascular grafts. Long-term and preclinical large animal examinations are required to evaluate the significance of this finding in terms of graft durability. Furthermore, evaluation of potential protective effects of antioxidative treatment, such as local binding of antioxidants to the implants, is warranted.

### AUTHOR CONTRIBUTIONS

Alexander Assmann and Payam Akhyari designed the research; Alexander Assmann, Vera Schmidt, Caroline Lepke, and Payam Akhyari analyzed the data; Vera Schmidt, Caroline Lepke, Yukiharu Sugimura, Anna Kathrin Assmann, and Mareike Barth performed the research; Alexander Assmann and Anna Kathrin Assmann wrote the manuscript; Artur Lichtenberg and Payam Akhyari critically reviewed the manuscript, Artur Lichtenberg provided resources; Alexander Assmann and Payam Akhyari supervised the project.

### ACKNOWLEDGMENTS

The authors gratefully acknowledge technical support by Gisela Müller. The generous support of the S. Bunnenberg Foundation to the Cardiovascular Research Facilities at Heinrich Heine University is greatly appreciated. Open Access funding enabled and organized by Projekt DEAL.

### DISCLOSURES

The authors declare no conflicts of interest.

### DATA AVAILABILITY STATEMENT

The data that support the findings of this study are available in the “Material and methods” section and Supplemental Material of this article.

### ORCID

Alexander Assmann  <https://orcid.org/0000-0003-3777-7772>

### REFERENCES

- Volpe M, Savoia C, De Paolis P, Ostrowska B, Tarasi D, Rubattu S. The renin-angiotensin system as a risk factor and therapeutic target for cardiovascular and renal disease. *J Am Soc Nephrol*. 2002;13(Suppl 3):S173-S178.
- Forstermann U, Xia N, Li H. Roles of vascular oxidative stress and nitric oxide in the pathogenesis of atherosclerosis. *Circ Res*. 2017;120(4):713-735.
- Miller JD, Chu Y, Brooks RM, Richenbacher WE, Pena-Silva R, Heistad DD. Dysregulation of antioxidant mechanisms contributes to increased oxidative stress in calcific aortic valvular stenosis in humans. *J Am Coll Cardiol*. 2008;52(10):843-850.

4. Branchetti E, Sainger R, Poggio P, et al. Antioxidant enzymes reduce DNA damage and early activation of valvular interstitial cells in aortic valve sclerosis. *Arterioscler Thromb Vasc Biol.* 2013;33(2):e66-e74.
5. Butany J, Collins MJ. Analysis of prosthetic cardiac devices: a guide for the practising pathologist. *J Clin Pathol.* 2005;58(2):113-124.
6. Laukkanen MO, Parascandolo A. Superoxide dismutase 1-3. In: Choi S, ed. *Encyclopedia of Signaling Molecules.* Springer International Publishing; 2018:5232-5238.
7. Xu D, Guo H, Xu X, et al. Exacerbated pulmonary arterial hypertension and right ventricular hypertrophy in animals with loss of function of extracellular superoxide dismutase. *Hypertension.* 2011;58(2):303-309.
8. Beyer AM, Raffai G, Weinberg BD, et al. Amelioration of salt-induced vascular dysfunction in mesenteric arteries of Dahl salt-sensitive rats by missense mutation of extracellular superoxide dismutase. *Am J Physiol Heart Circ Physiol.* 2014;306(3):H339-H347.
9. Assmann A, Zwirnmann K, Heidelberg F, et al. The degeneration of biological cardiovascular prostheses under pro-calcific metabolic conditions in a small animal model. *Biomaterials.* 2014;35(26):7416-7428.
10. Assmann A, Delfs C, Munakata H, et al. Acceleration of autologous in vivo recellularization of decellularized aortic conduits by fibronectin surface coating. *Biomaterials.* 2013;34(25):6015-6026.
11. Assmann A, Akhyari P, Delfs C, et al. Development of a growing rat model for the in vivo assessment of engineered aortic conduits. *J Surg Res.* 2012;176(2):367-375.
12. Munakata H, Assmann A, Poudel-Bochmann B, et al. Aortic conduit valve model with controlled moderate aortic regurgitation in rats: a technical modification to improve short- and long-term outcome and to increase the functional results. *Circ J.* 2013;77(9):2295-2302.
13. Pinto A, Immohr MB, Jahn A, et al. The extracellular isoform of superoxide dismutase has a significant impact on cardiovascular ischaemia and reperfusion injury during cardiopulmonary bypass. *Eur J Cardiothorac Surg.* 2016;50(6):1035-1044.
14. Dikalov S, Griendling KK, Harrison DG. Measurement of reactive oxygen species in cardiovascular studies. *Hypertension.* 2007;49(4):717-727.
15. Faraci FM, Didion SP. Vascular protection: superoxide dismutase isoforms in the vessel wall. *Arterioscler Thromb Vasc Biol.* 2004;24(8):1367-1373.
16. Folz RJ, Peno-Green L, Crapo JD. Identification of a homozygous missense mutation (Arg to Gly) in the critical binding region of the human EC-SOD gene (SOD3) and its association with dramatically increased serum enzyme levels. *Hum Mol Genet.* 1994;3(12):2251-2254.
17. Juul K, Tybjaerg-Hansen A, Marklund S, et al. Genetically reduced antioxidative protection and increased ischemic heart disease risk: the Copenhagen City Heart Study. *Circulation.* 2004;109(1):59-65.
18. Yamada H, Yamada Y, Adachi T, et al. Protective role of extracellular superoxide dismutase in hemodialysis patients. *Nephron.* 2000;84(3):218-223.
19. Chu Y, Alwahdani A, Iida S, Lund DD, Faraci FM, Heistad DD. Vascular effects of the human extracellular superoxide dismutase R213G variant. *Circulation.* 2005;112(7):1047-1053.
20. Iida S, Chu Y, Weiss RM, Kang YM, Faraci FM, Heistad DD. Vascular effects of a common gene variant of extracellular superoxide dismutase in heart failure. *Am J Physiol Heart Circ Physiol.* 2006;291(2):H914-H920.
21. Lund DD, Chu Y, Miller JD, Heistad DD. Protective effect of extracellular superoxide dismutase on endothelial function during aging. *Am J Physiol Heart Circ Physiol.* 2009;296(6):H1920-H1925.
22. Zhang B, Miller VM, Miller JD. Influences of sex and estrogen in arterial and valvular calcification. *Front Endocrinol (Lausanne).* 2019;10:622.
23. Guglielmo M, Fusini L, Muratori M, et al. Computed tomography predictors of structural valve degeneration in patients undergoing transcatheter aortic valve implantation with balloon-expandable prostheses. *Eur Radiol.* 2022;32:6017-6027.
24. Fukai T, Ushio-Fukai M. Superoxide dismutases: role in redox signaling, vascular function, and diseases. *Antioxid Redox Signal.* 2011;15(6):1583-1606.
25. Carlsson LM, Marklund SL, Edlund T. The rat extracellular superoxide dismutase dimer is converted to a tetramer by the exchange of a single amino acid. *Proc Natl Acad Sci U S A.* 1996;93(11):5219-5222.
26. Gongora MC, Qin Z, Laude K, et al. Role of extracellular superoxide dismutase in hypertension. *Hypertension.* 2006;48(3):473-481.
27. Tjang YS, van Hees Y, Korfer R, Grobbee DE, van der Heijden GJ. Predictors of mortality after aortic valve replacement. *Eur J Cardiothorac Surg.* 2007;32(3):469-474.
28. Nalluri N, Atti V, Munir AB, et al. Valve in valve transcatheter aortic valve implantation (ViV-TAVI) versus redo-surgical aortic valve replacement (redo-SAVR): a systematic review and meta-analysis. *J Interv Cardiol.* 2018;31(5):661-671.
29. Lee S, Levy RJ, Christian AJ, et al. Calcification and oxidative modifications are associated with progressive bioprosthetic heart valve dysfunction. *J Am Heart Assoc.* 2017;6(5):e005648.
30. Christian AJ, Lin H, Alferiev IS, et al. The susceptibility of bioprosthetic heart valve leaflets to oxidation. *Biomaterials.* 2014;35(7):2097-2102.
31. Assmann AK, Goschmer D, Sugimura Y, et al. A role for peroxisome proliferator-activated receptor gamma agonists in counteracting the degeneration of cardiovascular grafts. *J Cardiovasc Pharmacol.* 2021;79(1):e103-e115.
32. Legare JF, Lee TD, Ross DB. Cryopreservation of rat aortic valves results in increased structural failure. *Circulation.* 2000;102(19 Suppl 3):III75-III78.
33. Assmann A, Horstkotter K, Munakata H, et al. Simvastatin does not diminish the in vivo degeneration of decellularized aortic conduits. *J Cardiovasc Pharmacol.* 2014;64(4):332-342.
34. Chen Y, Zhao X, Wu H. Transcriptional programming in arteriosclerotic disease: a multifaceted function of the Runx2 (run-related transcription factor 2). *Arterioscler Thromb Vasc Biol.* 2021;41(1):20-34.
35. Richards J, El-Hamamsy I, Chen S, et al. Side-specific endothelial-dependent regulation of aortic valve calcification: interplay of hemodynamics and nitric oxide signaling. *Am J Pathol.* 2013;182(5):1922-1931.
36. Aikawa E, Nahrendorf M, Figueiredo JL, et al. Osteogenesis associates with inflammation in early-stage atherosclerosis evaluated by molecular imaging in vivo. *Circulation.* 2007;116(24):2841-2850.

37. Durham AL, Speer MY, Scatena M, Giachelli CM, Shanahan CM. Role of smooth muscle cells in vascular calcification: implications in atherosclerosis and arterial stiffness. *Cardiovasc Res.* 2018;114(4):590-600.
38. Guo H, Xu D, Kuroki M, et al. Kidney failure, arterial hypertension and left ventricular hypertrophy in rats with loss of function mutation of SOD3. *Free Radic Biol Med.* 2020;152:787-796.
39. Karlsson K, Marklund SL. Extracellular superoxide dismutase in the vascular system of mammals. *Biochem J.* 1988;255(1):223-228.
40. Marklund SL. Extracellular superoxide dismutase in human tissues and human cell lines. *J Clin Invest.* 1984;74(4):1398-1403.
41. Wolin MS. Extracellular superoxide dismutase depletion in hypertension unmasks a new role for angiotensin II in regulating Cu,Zn-superoxide dismutase activity. *Hypertension.* 2006;48(3):368-369.

## SUPPORTING INFORMATION

Additional supporting information can be found online in the Supporting Information section at the end of this article.

**How to cite this article:** Assmann A, Schmidt V, Lepke C, et al. Degeneration of biological heart valve grafts in a rat model of superoxide dismutase-3 deficiency. *The FASEB Journal.* 2022;36:e22591. doi:[10.1096/fj.202200727RR](https://doi.org/10.1096/fj.202200727RR)